Journal of Energy Storage 51 (2022) 104305

Contents lists available at ScienceDirect

Journal of Energy Storage

journal homepage: www.elsevier.com/locate/est

Steam-enhanced calcium-looping performance of limestone for thermochemical energy storage: The role of particle size

Juan Arcenegui-Troya [a,*], Pedro Enrique Sánchez-Jiménez [a,b,**], Antonio Perejón [a,b,**], José Manuel Valverde [c], Luis Allan Pérez-Maqueda [a,*]

[a] Instituto de Ciencia de Materiales de Sevilla, C. S. I. C.-Universidad de Sevilla, C. Américo Vespucio n 49, 41092 Sevilla, Spain
[b] Departamento de Química Inorgánica, Facultad de Química, Universidad de Sevilla, 41012 Sevilla, Spain
[c] Departamento de Electrónica y Electromagnetismo, Facultad de Física, Universidad de Sevilla, Avenida Reina Mercedes s/n, Sevilla 41012, Spain

ARTICLE INFO

Keywords:
Calcium looping
Thermochemical energy storage
Limestone

ABSTRACT

Steam injection has been proposed to attenuate the decay of CaO reactivity during calcium looping (CaL) under operating conditions compatible with carbon capture and storage. However, it is yet unknown whether the perceived advantages granted by steam hold under the distinct operating conditions required for the integration of the CaL process as a thermochemical energy storage system in Concentrating Solar Power Plants (CaL-CSP). Here, we study the influence of steam in conditions compatible with a CaL-CSP scheme and assess its impact when injected only during one stage; either calcination or carbonation, and also when it is present throughout the entire loop. The results presented here demonstrate that steam boosts the CaO multicycle performance in a CO_2 closed loop to attain residual conversion values similar to those achieved at moderate temperatures under inert gas. Moreover, it is found that the enhancement in multicycle activity is more pronounced for larger particles.

1. Introduction

Climate change mitigation requires a global coordination to reduce CO_2 emissions. Given that electricity generation based on fossil fuel combustion is responsible for the largest share of these emissions, the massive deployment of renewable energy sources is crucial to cope with this challenge. Nonetheless, the dependence of renewable energy sources on weather variability, such as the intermittency of solar radiation, makes it difficult to match power supply and demand [1,2]. To overcome these difficulties, the development of efficient, economical and environmentally friendly energy storage systems is required. With regards to this, the system based on the reversible calcination/carbonation reaction of $CaCO_3$/CaO, known as calcium looping (CaL) process, is postulated as a promising technology for the storage of concentrated solar power at high temperature (CaL-CSP) [3–5].

In the CaL-CSP integration, solar radiation would be utilized to drive the endothermic decomposition of $CaCO_3$ [4,5]. The products, CaO and CO_2, are stored separately and brought back together to produce the reverse exothermic reaction, releasing the energy on demand. Afterwards, the regenerated $CaCO_3$ would be used in a store and release cycle [6]. Some advantages of the CaL-CSP technology, as compared with other energy storage systems currently in use, include long term storage with negligible thermal losses as well as higher energy densities (3.2 GJ/m^3 as compared to 0.8 GJ/m^3 for molten salts) [4,7]. Besides, CaO natural precursors such as limestone and dolomite are cheap, non-toxic and widely abundant [8–10].

Among the different CaL-CSP schemes proposed, calcination in inert gas is often proposed to be carried out at about 750 °C [11,12]. On the other hand, carbonation temperature largely depends on the partial pressure of CO_2 employed [13]. In pure CO_2, the carbonation temperature can be efficiently conducted at 850 °C, attaining large CaO conversions in short residence times [4,5]. However, calcining in inert gas requires separating the CO_2 from the mixture of gases released from the calciner. This step substantially increases the cost and complexity of this technology [14,15]. This issue would be circumvented if both calcination, carbonation and power generation were conducted in CO_2 [16].

* Corresponding authors.
** Corresponding authors at: Departamento de Química Inorgánica, Facultad de Química, Universidad de Sevilla, 41012 Sevilla, Spain.
E-mail addresses: jjarcenegui@icmse.csic.es (J. Arcenegui-Troya), pedro.enrique@icmse.csic.es (P.E. Sánchez-Jiménez), antonio.perejon@icmse.csic.es (A. Perejón), maqueda@icmse.csic.es (L.A. Pérez-Maqueda).

https://doi.org/10.1016/j.est.2022.104305
Received 8 November 2021; Received in revised form 1 February 2022; Accepted 21 February 2022
Available online 8 March 2022

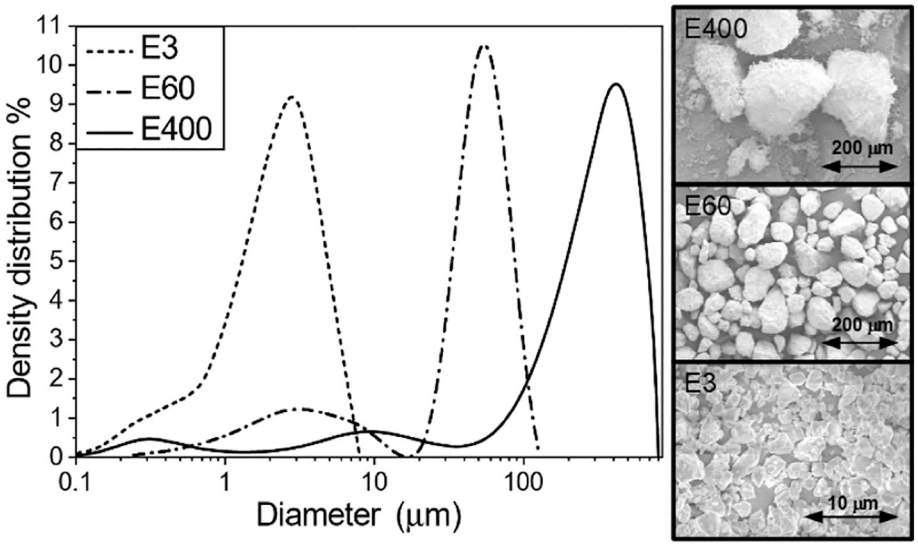

Fig. 1. SEM images and PSD of the three limestone samples tested.

However, in presence of CO_2 the calcination has to be carried out at higher temperatures (~950 °C) [12], which is known to adversely affects the activity of CaO-based sorbents [17,18]. A possible alternative to separating CO_2 from the mixture of gases leaving in the calcineris to couple the CaL-CSP process for TCES with a CO_2 emitting industry [11].

A major drawback of this technology is the sintering-induced deactivation of CaO, which is markedly enhanced at the high temperatures and CO_2-rich environment required to promote heat-to-power efficiency [18,19]. The loss in reactivity is mainly attributed to two factors; pore plugging and sintering [20–22]. Pore plugging occurs when a $CaCO_3$ layer is quickly formed on the CaO particle's surface during carbonation, blocking the pores and hindering CO_2 from reaching the unreacted CaO core [20,23]. In practice, the progressive loss in reactivity could be offset by replacing the spent sorbent with fresh CaO, however at the expense of increasing costs and energy penalties [24]. Much research in the last years have been devoted to devise strategies to mitigate or even prevent the deactivation of CaO. The strategies proposed to this end range from the use of thermally stable additives to thermal and chemical pretreatments [8,22,25–27].

Steam injection has been explored as a method to reduce CaO deactivation in studies mainly focussed on the application of CaL to carbon capture and storage (CCS) [28–37]. However, the conclusions of these studies do not lack controversy. Most authors have reported a beneficial influence of steam [28,29,38]. Some even conclude that the impact of steam is positive no matter if it is injected during carbonation, calcination or in both stages [28,29]. On the other hand, as it is generally accepted that steam promotes sintering [39,40], some authors have reported a negative or neutral impact on the multicycle performance of CaO [36,37]. Homsy et al. have recently pointed out that the microstructure of the calcium precursor plays an important role, finding a negative influence of steam on CaO derived from marble [35]. Some authors assume that steam improves carbonation during the fast reaction-controlled regime because of the formation of $Ca(OH)_2$, which is more reactive to CO_2 than CaO [41,42]. However, $Ca(OH)_2$ formation is not thermodynamically favoured at the temperatures used for carbonation in CCS conditions (~650 °C), which cast doubts on this argument; rather, it has been observed that steam enhances conversion during the diffusion-controlled regime [30,43], which has been

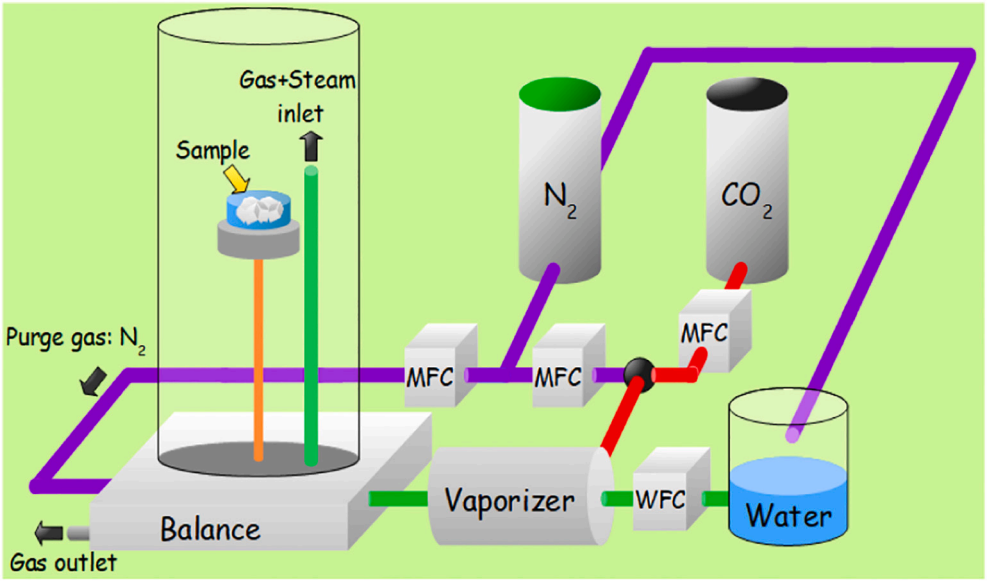

Fig. 2. Experimental setup used for the multicycle tests conducted.

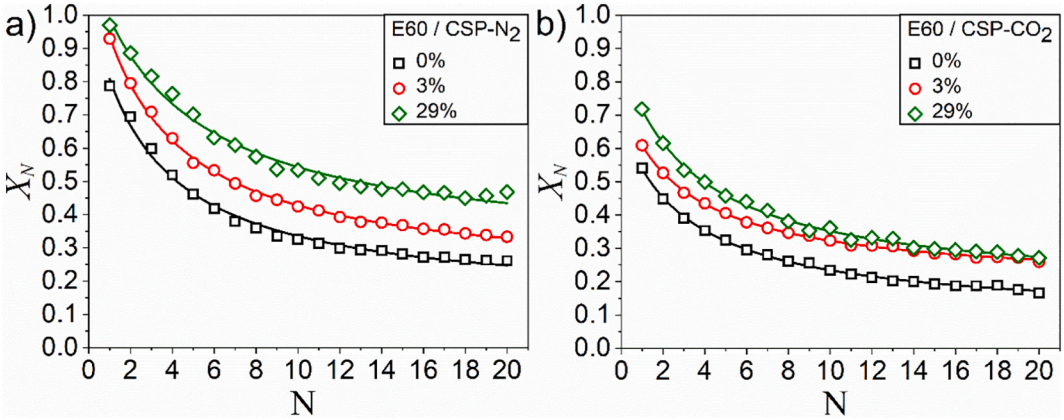

Fig. 3. Effective conversion measured as a function of the cycle number in tests conducted under a) CSP-N_2 and b) CSP-CO_2 conditions. Solid lines represent the best fitting of Eq. (2) to the data.

attributed to the formation of OH^- after H_2O dissociation [31]. Besides, recent results have demonstrated that steam injection during calcination allows reducing the temperature required to calcine limestone in conditions compatible with CaL-CSP, which would lead to important energy savings [44]. This reduction has been attributed to different causes, such as a promotion of the heat transfer coefficient due to the higher thermal conductivity of steam [45–47], a catalytic effect for steam [48–50] or enhanced surface reactivity [51–53]. The decrease of the calcination temperature minimize the sintering-induced deactivation, improving the multicycle performance of CaO [44]. Besides, the CaO resulting from calcination in the presence of steam exhibits a distinct microstructure, with larger pores less susceptible to pore plugging, further facilitating subsequent carbonation [34,44].

Owing to the different experimental conditions employed, the conclusions of the aforementioned works cannot be directly extrapolated to a potential CaL-CSP integration. Thus, further research is needed to clarify the impact of steam under the distinct conditions demanded by a CaL-CSP integration. In the present work, we study the influence of steam on the CaO multicycle performance under different operation conditions compatible with a CaL-CSP integration. Moreover, the influence of steam has been analysed as depending on the particle size, as it is a relevant parameter in the practical application as it affects critically the material flowability and CaO multicycle performance [54–56].

2. Materials and methods

Limestone samples supplied by Staubtechnik GmbH (Germany) were used in this study (~99.9% $CaCO_3$). Given the high purity, 100% $CaCO_3$ would be assumed in all relevant calculations. Three samples with well-defined particle size distributions (PSD), selected by aerodynamics classification, have been tested. Fig. 1 shows a SEM image and the PSD of each sample. The PSDs exhibit a peak around 3 μm, 60 μm and 400 μm. From now on we will refer to these samples as E3, E60 and E400, respectively. The micrographs were taken with a scanning electron microscope (SEM) HITACHI S4800 and the PSD were measured using a laser diffractometer Mastersizer Malvern Instruments.

Multicycle experiments were run in a thermogravimetric analyzer (TGA) LINSEIS STA PT 1600 coupled to a steam generator. Fig. 2 shows a scheme of the experimental setup. Water was injected from a tank through a water flow controller (WFC) BRONKHORST LIQUI-FLOW L13V12 up to a vaporizer. N_2 was used to pressurize the water tank and also as a purge gas. The steam produced in the vaporizer was mixed with the carrier gas and the mixture was circulated to the TGA through a transfer line kept at 165 °C to avoid condensation. Gas flow was controlled using mass flow controllers (MFC). Depending on the conditions studied, the carrier gas was N_2 or CO_2.

Two distinct types of experimental conditions were tested, both compatible with elsewhere proposed CaL-CSP integrations [4,6]. Firstly, calcination was conducted in a mixture of H_2O/N_2 at 730 °C, whereas carbonation was carried out in a mixture of H_2O/CO_2 at 850 °C. We will refer to these conditions as CSP-N_2. Secondly, CSP-CO_2 conditions consisted of cycles in which calcination and carbonation were carried out at 950 °C and 850 °C, respectively, but maintaining the same H_2O/CO_2 atmosphere during the entire experiment. Steam in different proportions, 0%, 3% and 29% vol, was continuously injected throughout these experiments. These values were selected to reflect both low (attainable with saturated gas) and high steam concentrations (requiring water injection).

In all cases the multicycle tests were initiated with a heating ramp up to the calcination temperature. Once calcination was fully attained, the temperature was either increased or decreased, depending on whether the conditions used were CSP-N_2 or CSP-CO_2, to the reach carbonation temperature. Carbonation was carried out for 5 min to simulate the residence times required in practice [4]. Afterwards, the temperature was changed to the value employed for calcination and the cycle was repeated 19 times.

The impact of cycling on the samples' microstructure under the different conditions studied was analysed using the above-mentioned electron microscope. Previously, the samples were gold-coated utilizing an Emitech K550 Telstar sputter-coating machine (30 s, 30 mA).

Pore size distribution and S_{BET} surface area of CaO after one calcination was determined by N_2 physisorption analysis. The experiment was performed ex-situ in order to have enough mass of material for reliable characterization. Thus, 1 g of $CaCO_3$ was calcined in a tubular furnace in conditions that mimicked those used in the multicycle experiments conducted in the TGA. First, the sample was heated at 10 °C/min up to 730 °C, and the temperature was maintained constant for 30 min to carry out the calcination either in 100% N_2 or in a H_2O/N_2 mixture. Water was injected into the tubular furnace through a peristaltic pump (~0.2 ml/s). Before the physisorption analysis, the samples were degassed at 350 °C for 2 h.

3. Results and discussion

3.1. Influence of continuous steam injection on the CaO multicyclic activity

Fig. 3 shows the evolution of effective conversion measured for sample E60 with the cycle number under CSP-N_2 and CSP-CO_2 conditions, depending on the different steam concentrations employed. Effective conversion is defined as:

$$X_N = \frac{(m_N - m)\cdot W_{CaO}}{m\cdot W_{CO2}} \quad (1)$$

Table 1
Best-fitting parameters of Eq. (2) to the data shown in Fig. 3.

Steam dilution	CSP-N_2			CSP-CO_2		
	X_r	k	R^2	X_r	k	R^2
0%	0.13 ± 0.01	0.31 ± 0.03	0.992	0.09 ± 0.01	0.28 ± 0.02	0.997
3%	0.20 ± 0.01	0.31 ± 0.01	0.998	0.19 ± 0.01	0.35 ± 0.02	0.998
29%	0.28 ± 0.02	0.26 ± 0.04	0.987	0.17 ± 0.01	0.29 ± 0.02	0.996

Table 2
Best-fitting parameters of Eq. (2) to the data shown in Fig. 6.

CSP-N_2 conditions	X_r	k	R^2
0% H_2O	0.13 ± 0.01	0.31 ± 0.03	0.992
3% H_2O in carbonation	0.14 ± 0.01	0.34 ± 0.02	0.998
3% H_2O in calcination	0.19 ± 0.01	0.25 ± 0.02	0.995
3% H_2O in calcination and carbonation	0.20 ± 0.01	0.31 ± 0.01	0.998

where m_N is the sample mass at the end of the carbonation stage during the cycle N, m is the sample mass before carbonation, and W_{CaO} and W_{CO2} the molar masses of CaO and CO_2, respectively.

As expected, effective conversion decreases in all cases with the cycle number. It is clear that the conversion values attained in CSP-CO_2 conditions are consistently lower than in CSP-N_2. This may be ascribed to the harsher calcination conditions used in the CSP-CO_2 tests. In CO_2-rich atmosphere, a temperature over 950 °C is required to fully calcine the sample in 5 min. Also, it is widely known that CaO sintering is aggravated in the presence of CO_2 [17,40,57]. Data depicted in Fig. 3 can be reasonably well fitted by the following equation [58]:

$$X_N = X_r + \frac{X_1}{k(N-1) + (1 - X_r/X_1)^{-1}} \quad (2)$$

being X_r the residual conversion, which represents the asymptotical value toward which conversion converges after many cycles. X_1 is the effective conversion at the first cycle and k is known as deactivation constant. The best fitting curves are represented as solid lines in Fig. 3 and the best fitting parameters are collected in Table 1.

According to the results plotted in Fig. 3 and the residual conversion values shown in Table 1, it can be concluded that steam injection promotes CaO multicycle reactivity. However, the net effect largely depends on reaction conditions; in CSP-N_2 the CaO conversion at each cycle noticeably increases with the concentration of steam. On the other hand, under CSP-CO_2 conditions, the values of residual conversion attained with 3% H_2O and 29% H_2O are roughly similar; thereby indicating no further improvement can be obtained by raising the amount of steam injected over 3% vol.

Since in the real application the material is expected to be recycled hundreds of times, the most representative parameter to assess the multicycle performance is the residual conversion. The parameters collected in Table 2 can be employed to estimate the accumulated stored energy (ASE) up to the Nth cycle as follows:

$$ASE(\mathrm{kJ/kg}) = \sum_{i=1}^{N} \frac{1}{W_{CaCO_3}} \left(X_r + \frac{X_1}{k(i-1) + (1 - X_r/X_1)^{-1}} \right) \cdot \Delta H \quad (3)$$

where $\Delta H = 178$ kJ/mol is the enthalpy of carbonation and W_{CaCO3} is the molar mass of $CaCO_3$ expressed in kg/mol. The results of this calculation are plotted in Fig. 4a for an arbitrary large number of 1000 cycles. This graph illustrates how a slight enhancement in the residual conversion leads to a significant increase in the *ASE*.

It is remarkable that the injection of just 3% H_2O in CSP-CO_2 conditions results in long-term ASE substantially larger than achieved in CSP-N_2 conditions in the absence of steam. This is particularly relevant as CSP-CO_2 operation conditions were proposed to avoid the need to separate N_2 and CO_2, at the expense of aggravated decay due to the higher calcination temperatures. These results show the addition of a small amount of steam improves the potential of the closed CO_2 loop

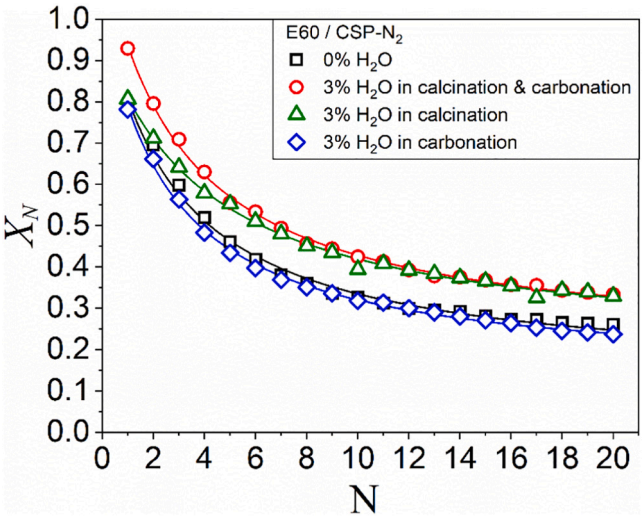

Fig. 5. Effective conversion values obtained in multicycle experiments where steam was injected in different stages of the CaL process.

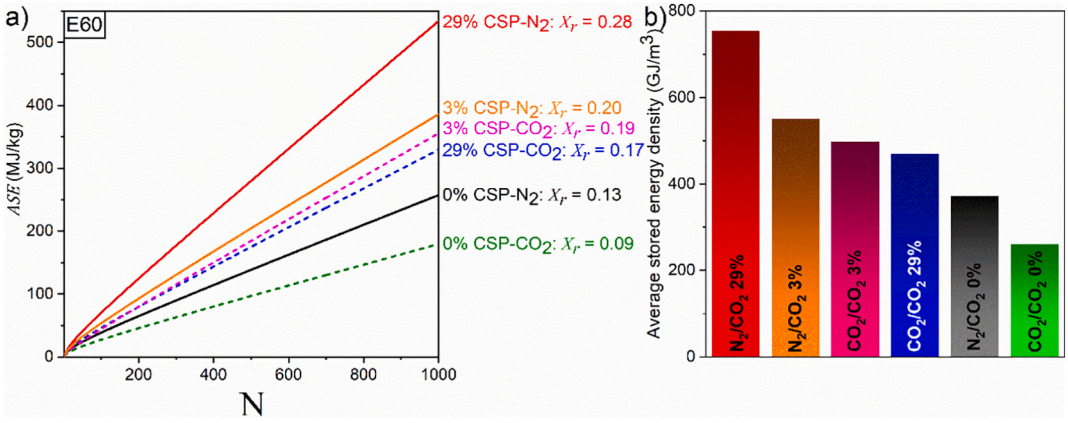

Fig. 4. a) Accumulated stored energy as a function of the cycle number. Data represented have been calculated using the best-fitting parameters shown in Table 1 and Eq. (3). b) Average stored energy density after 1000 cycles.

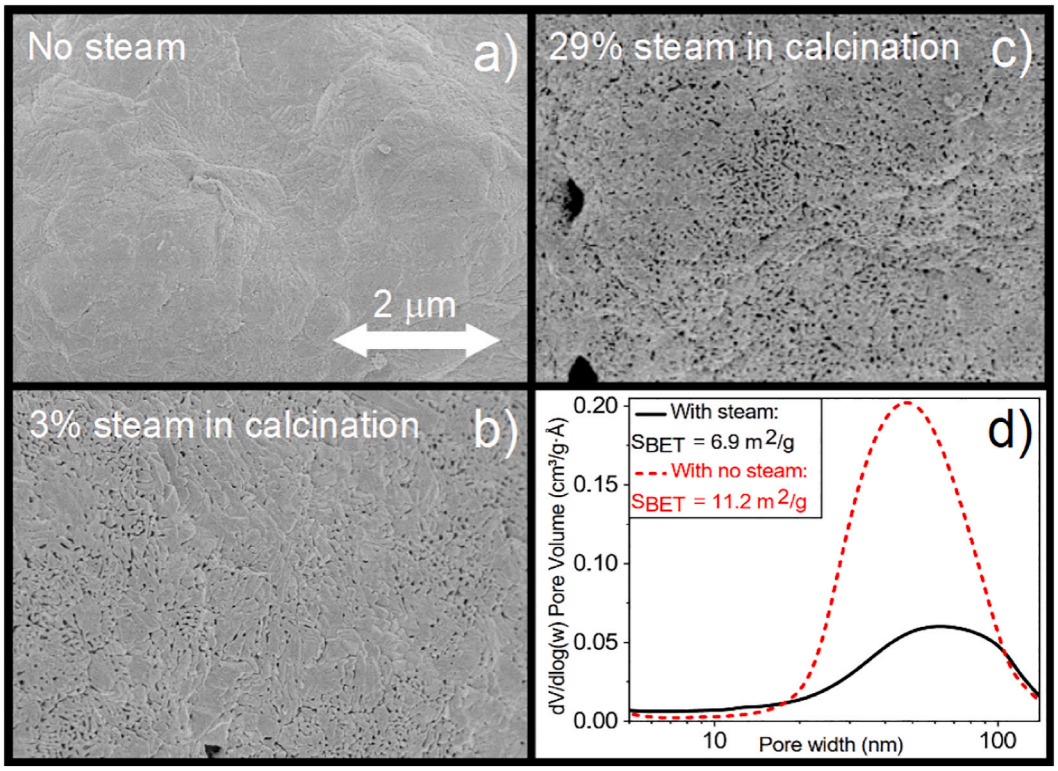

Fig. 6. SEM micrographs of the surface of two CaO particles, produced after 20 cycles (CSP-N_2 conditions) conducted with a) no steam, b) 3% H_2O and c) 29% H_2O added in the calcination stage. d) Pore size distribution and BET surface measurements of CaO after one calcination.

integration. Fig. 4b shows the average stored energy density after 1000 cycles for the different conditions tested. These values were calculated assuming a density for $CaCO_3$ of 2711 kg/m^3.

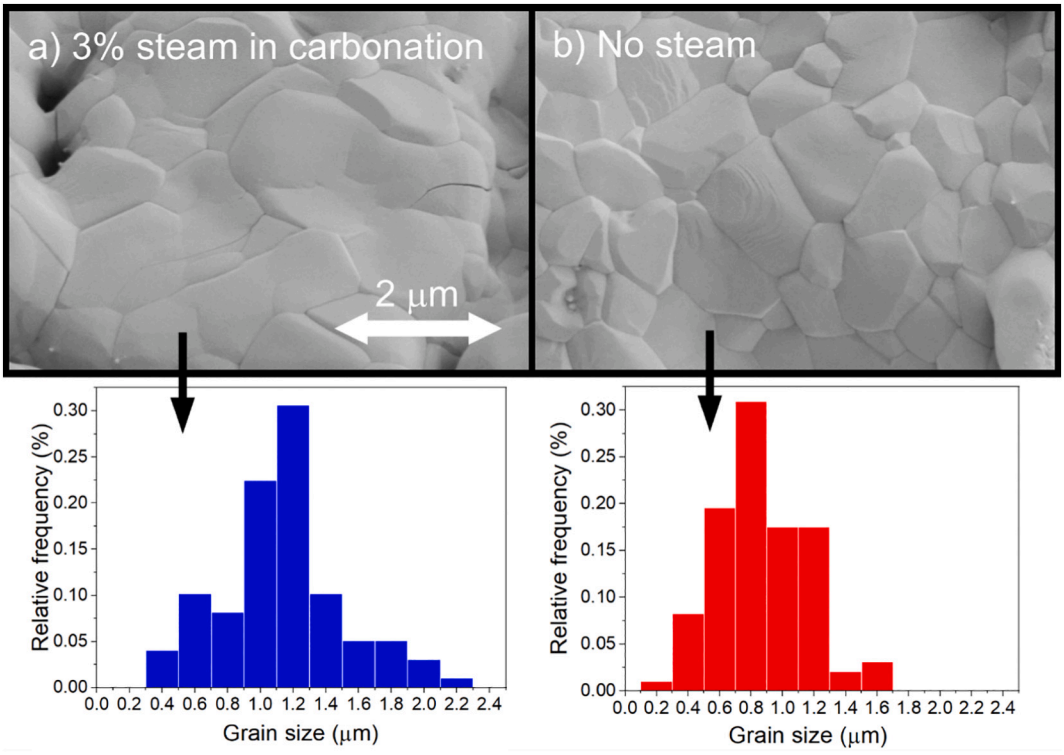

Fig. 7. SEM micrographs of the surface of two $CaCO_3$ particles, produced after 20 cycles, ending in carbonation (CSP-N_2 conditions), conducted with a) 3% H_2O in carbonation and b) no steam. The histograms with the grain size distribution corresponding to each sample are also shown.

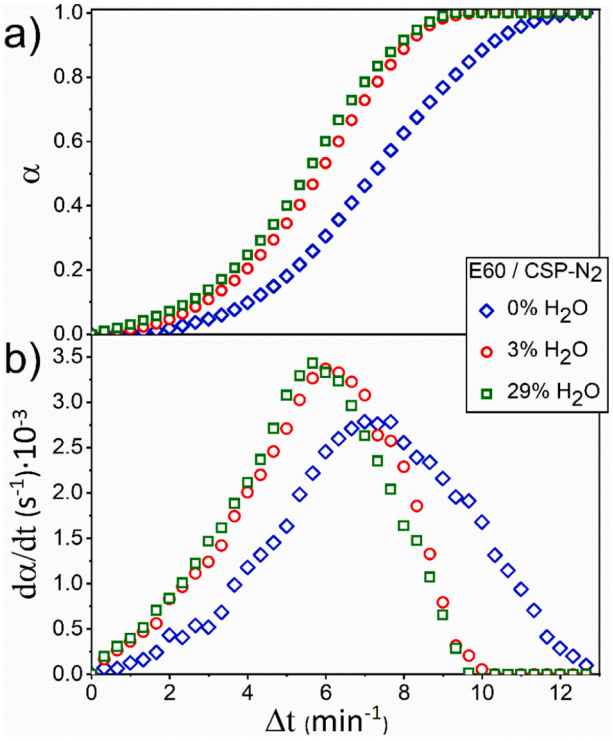

Fig. 8. Extent of reaction during the first calcination as a function of time for different contents of steam.

3.2. *Effect of steam injected on a single stage (either calcination or carbonation)*

To better comprehend the mechanism of the steam-induced improvement of the CaO multicycle activity, we conducted multicycle tests in which steam injection was restricted to either calcination or carbonation. Tests were carried out under CSP-N_2 conditions, with the addition of 3% H_2O. The results are shown in Fig. 5 and the best fitting parameters of Eq. (2) to these data are listed in Table 2. It seems clear from the comparison that the presence of steam solely during the carbonation has a negligible effect on CaO multicycle performance. On the other hand, steam injection during the calcination stage leads to a substantial improvement of the multicycle activity, roughly similar to what is obtained when water is present during the entire process. Arguably, it can be concluded that the presence of water during the calcination of $CaCO_3$ is the key to the improvement.

The SEM images in Fig. 6b and c respectively correspond to the surface of CaO particles subjected to 20 cycles, carried out in CSP-N_2 conditions with 3% and 29% H_2O added during calcination. The samples exhibit a distinct texture, composed of sizable pores largely absent on the CaO particles obtained when calcination was carried out in the absence of steam (Fig. 6a).

Table 3
Best-fitting parameters of Eq. (2) to the data shown in Fig. 8.

CSP-CO_2 conditions	X_r	k	R^2
E3 0%	0.18 ± 0.01	0.45 ± 0.02	0.989
E3 3%	0.23 ± 0.01	0.35 ± 0.01	0.993
E60 0%	0.09 ± 0.01	0.28 ± 0.02	0.998
E60 3%	0.19 ± 0.01	0.35 ± 0.02	0.998
E400 0%	0.05 ± 0.01	0.33 ± 0.02	0.998
E400 3%	0.18 ± 0.01	0.33 ± 0.02	0.996

Fig. 6d shows a porosimetry analysis of the nascent CaO after a single calcination cycle in two different atmospheres: 100% N_2 and a H_2O/N_2 mixture. BET surface values are provided in the legend. As it might be observed, there is a slight shift toward larger pores when calcination is conducted in the presence of steam. However, the BET surface values are smaller. Therefore, it could be argued that steam injected during calcination favour the creation of larger pores less susceptible to pore plugging, which explains the higher values of conversion attained. At the same time, the enhanced diffusivity of CO_2 through the larger pores offsets the reduced surface area available [28].

Fig. 7 shows SEM micrographs of the surface of the $CaCO_3$ particles after 20 calcination and carbonation cycles, ending in carbonation, conducted under different conditions. The SEM image in Fig. 7a corresponds to the surface of a $CaCO_3$ particle subjected to multicycle tests conducted with the addition to 3% steam during the carbonation stage, while the SEM image in Fig. 7b corresponds to a sample cycled without steam addition in the carbonation stage. The mineralising effect of steam can be appreciated in the larger grains in the former sample. Histograms with the grain size distribution, constructed using five SEM photos to ensure its representativeness, are also shown.

Several prior works have also shown that steam can accelerate calcination kinetics [59]. This is demonstrated in the plots included in Fig. 8, where the extent of reaction, measured during the first calcination, is plotted as a function of time for different contents of steam. This capability of steam to speed up the calcination could be exploited to decrease the temperature required to calcine limestone in the short residence times required in practice (~10 min), which would allow to save energy and help prevent high temperature-induced sintering [44].

3.3. *Influence of particle size on steam enhancement*

Particle size has a decisive influence on the multicycle performance

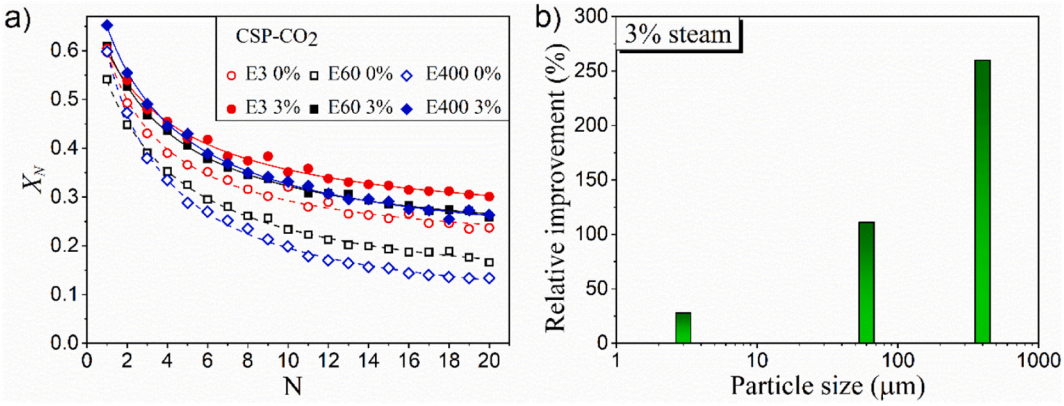

Fig. 9. a) Multicycle CaO conversion as a function of the cycle number for the different samples studied. Open symbols correspond to experiments conducted with no steam. Solid lines represent the best fit of Eq. (2) to the experimental data. b) Relative improvement as a function of the particle size.

of CaO [54]. The multicycle CaO conversion values obtained for particles with different particle sizes are shown in Fig. 9a. These experiments were carried out under CSP-CO_2 conditions, as the results in previous sections showed that steam-injection makes more attractive the operation in a closed loop to avoid costly gas separation procedures. For each particle size, the multicyclic activity was assessed in the absence of steam and with continuous injection of 3% H_2O. The best fitting parameters of the experimental data to Eq. (2) are included in Table 3. Fig. 9b shows the relative increase in the residual conversion as a function of the particle size. The observed CaO conversion values decrease with the particle size. At the CaL-CSP carbonation conditions here employed, the $CaCO_3$ layer rapidly forming on the surface of the particles prevents the CO_2 from reaching the unreacted core of the particle [57]. For the small particles, the ratio between the surface area and the volume is higher; therefore, the fraction of CaO that remains occluded and inactive during the carbonation stage is necessarily smaller. Thus, the correspondingly higher values of conversion. The effect is more significant for particles sizes below 15 μm [54]. This correlation between particle size and conversion is evident in the plots in Fig. 9a. Nonetheless, the use of small particles on an industrial scale would entail some drawbacks. The residence time of a particle in a cyclone strongly depends on its size, and collection efficiency significantly decays for particle sizes below 10 μm [60,61]. Moreover, powder flowability at high temperature is significantly hindered as particle size is decreased [55,56]. On the other hand, albeit several types of reactors, such as entrained cyclone or stacked bed-rotary kiln have been considered, often the thermochemical energy storage of concentrated solar power is proposed to be performed in fluidized bed reactors [62–64]. It has been found that the optimum size in pilot plants based on fluidized bed reactors ranges from 100 μm to 300 μm [65,66]. Thereby the interest in assessing the effect of steam on the multicycle activity displayed by large particles. As seen in Fig. 9a, the multicycle activity of sample E400 is notably improved by the steam addition, increasing its residual conversion from 0.05 ± 0.01 to 0.18 ± 0.01. Actually, the multicyclic performance of the sample E400 in the presence of steam improves the activity exhibited by E3 with no steam. These results demonstrate that the addition of steam would allow the use of larger particles while limiting the reduction in CaO multicycle conversion.

4. Conclusions

In this work, we have studied the influence of steam on the multicycle performance of limestone samples as depending on the particle size, under experimental conditions compatible with a CaL-CSP integration. The results demonstrate that steam is beneficial when it is injected throughout the cycle or just during the calcination stage, while the effect is neutral when it is added solely during the carbonation stage. During calcination, steam promotes a more porous microstructure on the nascent CaO. The impact of calcining in the presence of steam during calcination is more beneficial for larger particles, more susceptible to significant pore-plugging deactivation.

As expected, due to the harsh conditions endured in CSP-CO_2 tests, where calcination was carried out under high CO_2 concentration, the values of conversion attained in CSP-N_2 conditions (calcination under N_2 at moderate temperature) are higher. Conversely to what occurs in CSP-CO_2 tests, where the improvement caused by steam seems to reach a limit, the positive effect of steam under CSP-N_2 is further promoted as the concentration of steam is increased. Remarkably, the value of residual conversion achieved with 3% steam in CSP-CO_2 tests is higher than that obtained in tests conducted under CSP-N_2 with no steam. Thus, using steam would allow overcoming the drawbacks associated with the deactivation of the material as a consequence of pore plugging, which would allow operating the CaL-CSP integration in a closed CO_2 cycle working in these latter conditions and thus circumventing the technical issues derived from to CO_2/N_2 gas separation.

Remarkably, calcination under 3% steam boosts the multicycle activity of limestone particles with sizes around 400 μm, whose performance under dry conditions is seriously limited by pore plugging, obtaining values of conversion similar to those achieved with the smallest particles used in this work when no steam is injected. Thus the injection of steam in the calcination stage would serve to use limestone powders of relatively large particle size, best suited for the practical application as compared with fine powders.

CRediT authorship contribution statement

Juan Arcenegui-Troya: Conceptualization, Formal analysis, Investigation, Writing - Original Draft, Visualization. **Pedro Enrique Sánchez-Jiménez**: Conceptualization, Resources, Writing - Original Draft, Visualization, Supervision. **Antonio Perejón**: Conceptualization, Resources, Visualization, Supervision. **José Manuel Valverde**: Conceptualization. **Luis Allan Pérez-Maqueda**: Conceptualization, Resources, Visualization, Supervision, Funding acquisition.

Declaration of competing interest

The authors declare that they have no known competing financial interests or personal relationships that could have appeared to influence the work reported in this paper.

Acknowledgements

This work has been supported by the Spanish Government Agency Ministerio de Economía y Competitividad-FEDER (contracts CTQ2017-83602-C2-1-R and -2-R) and Junta de Andalucía and Universidad de Sevilla (Programa Operativo FEDER Andalucía 2014–2020, projects P18-FR-1087 and US-1262507). We acknowledge the funding received by the European Union's Horizon 2020 research and innovation programme under grant agreement No. 727348, project SOCRATCES. Financial support received from Junta de Andalucía-Consejería de Economía, Conocimiento, Empresas y Universidad via a postdoctoral fellowship with reference DOC_00044 is also acknowledged.

References

[1] X. Peng, T.W. Root, C.T. Maravelias, Storing solar energy with chemistry: the role of thermochemical storage in concentrating solar power, Green Chem. 19 (2017) 2247–2438, https://doi.org/10.1039/c7gc00023e.
[2] H.A. Behabtu, M. Messagie, T. Coosemans, M. Berecibar, K.Anlay Fante, A. A. Kebede, J.Van Mierlo, A review of energy storage technologies' application potentials in renewable energy sources grid integration, Sustainability 12 (2020) 10511, https://doi.org/10.3390/su122410511.
[3] SOCRATCES (SOlar Calcium-looping integRAtion for ThermoChemical Energy Storage), n.d. https://socratces.eu/. (Accessed 23 November 2020).
[4] R. Chacartegui, A. Alovisio, C. Ortiz, J.M. Valverde, V. Verda, J.A. Becerra, Thermochemical energy storage of concentrated solar power by integration of the calcium looping process and a CO2 power cycle, Appl. Energy (2016) 589–605, https://doi.org/10.1016/j.apenergy.2016.04.053.
[5] B. Sarrion, J.M. Valverde, A. Perejon, L. Perez-Maqueda, P.E. Sanchez-Jimenez, On the multicycle activity of natural limestone/dolomite for thermochemical energy storage of concentrated solar power, Energy Technol. 4 (2016) 1013–1019, https://doi.org/10.1002/ente.201600068.
[6] C. Ortiz, M.C. Romano, J.M. Valverde, M. Binotti, R. Chacartegui, Process integration of calcium-looping thermochemical energy storage system in concentrating solar power plants, Energy 155 (2018) 535–551, https://doi.org/10.1016/j.energy.2018.04.180.
[7] P. Pardo, A. Deydier, Z. Anxionnaz-Minvielle, S. Rougé, M. Cabassud, P. Cognet, A review on high temperature thermochemical heat energy storage, Renew. Sust. Energ. Rev. 32 (2014) 591–610, https://doi.org/10.1016/j.rser.2013.12.014.
[8] M. Erans, V. Manovic, E.J. Anthony, Calcium looping sorbents for CO2 capture, Appl. Energy 180 (2016) 722–742, https://doi.org/10.1016/j.apenergy.2016.07.074.
[9] I. Ortega-Fernández, N. Calvet, A. Gil, J. Rodríguez-Aseguinolaza, A. Faik, B. D'Aguanno, Thermophysical characterization of a by-product from the steel industry to be used as a sustainable and low-cost thermal energy storage material, Energy 89 (2015) 601–609, https://doi.org/10.1016/j.energy.2015.05.153.
[10] J. Arcenegui-Troya, P.E. Sánchez-Jiménez, A. Perejón, J.M. Valverde, R. Chacartegui, L.A. Pérez-Maqueda, Calcium-looping performance of biomineralized CaCO3for CO2Capture and thermochemical energy storage, Ind.

Eng. Chem. Res. 59 (2020) 12924–12933, https://doi.org/10.1021/acs.iecr.9b05997.
[11] C. Tregambi, F. Di Lauro, F. Montagnaro, P. Salatino, R. Solimene, 110th anniversary: calcium looping coupled with concentrated solar power for carbon capture and thermochemical energy storage, Ind. Eng. Chem. Res. 58 (2019) 21262–21272, https://doi.org/10.1021/acs.iecr.9b03083.
[12] M. Bailera, S. Pascual, P. Lisbona, L.M. Romeo, Modelling calcium looping at industrial scale for energy storage in concentrating solar power plants, Energy 225 (2021), 120306, https://doi.org/10.1016/j.energy.2021.120306.
[13] S. Pascual, P. Lisbona, M. Bailera, L.M. Romeo, Design and operational performance maps of calcium looping thermochemical energy storage for concentrating solar power plants, Energy 220 (2021), 119715, https://doi.org/10.1016/j.energy.2020.119715.
[14] A. Fernández-Barquín, C. Casado-Coterillo, Á. Irabien, Separation of CO2-N2 gas mixtures: membrane combination and temperature influence, Sep. Purif. Technol. 188 (2017) 197–205, https://doi.org/10.1016/j.seppur.2017.07.029.
[15] M. Chawla, H. Saulat, M. Masood Khan, M. Mahmood Khan, S. Rafiq, L. Cheng, T. Iqbal, M.I. Rasheed, M.Z. Farooq, M. Saeed, N.M. Ahmad, M.B. Khan Niazi, S. Saqib, F. Jamil, A. Mukhtar, N. Muhammad, Membranes for CO2 /CH4 and CO2/N2 gas separation, Chem. Eng. Technol. 43 (2020) 184–199, https://doi.org/10.1002/ceat.201900375.
[16] A. Alovisio, R. Chacartegui, C. Ortiz, J.M. Valverde, V. Verda, Optimizing the CSP-calcium looping integration for thermochemical energy storage, Energy Convers. Manag. 136 (2017) 85–98, https://doi.org/10.1016/j.enconman.2016.12.093.
[17] B. Sarrión, A. Perejón, P.E. Sánchez-Jiménez, L.A. Pérez-Maqueda, J.M. Valverde, Role of calcium looping conditions on the performance of natural and synthetic Ca-based materials for energy storage, J. CO2 Util. 28 (2018) 374–384, https://doi.org/10.1016/j.jcou.2018.10.018.
[18] A.A. Scaltsoyiannes, A.A. Lemonidou, On the factors affecting the deactivation of limestone under calcium looping conditions: a new comprehensive model, Chem. Eng. Sci. 243 (2021) 116797, https://doi.org/10.1016/j.ces.2021.116797.
[19] V. Manovic, J.P. Charland, J. Blamey, P.S. Fennell, D.Y. Lu, E.J. Anthony, Influence of calcination conditions on carrying capacity of CaO-based sorbent in CO2 looping cycles, Fuel 88 (2009) 1893–1900, https://doi.org/10.1016/j.fuel.2009.04.012.
[20] M. Benitez-Guerrero, B. Sarrion, A. Perejon, P.E. Sanchez-Jimenez, L.A. Perez-Maqueda, J. Manuel Valverde, Large-scale high-temperature solar energy storage using natural minerals, Sol. Energy Mater. Sol. Cells 168 (2017) 14–21, https://doi.org/10.1016/j.solmat.2017.04.013.
[21] J.M. Valverde, P.E. Sanchez-Jimenez, L.A. Perez-Maqueda, Ca-looping for postcombustion CO2 capture: a comparative analysis on the performances of dolomite and limestone, Appl. Energy 138 (2015) 202–215, https://doi.org/10.1016/j.apenergy.2014.10.087.
[22] B. Sarrion, P.E. Sanchez-Jimenez, A. Perejon, L.A. Perez-Maqueda, J.M. Valverde, Pressure effect on the multicycle activity of natural carbonates and a Ca/Zr composite for energy storage of concentrated solar power, ACS Sustain. Chem. Eng. 6 (2018) 7849–7858, https://doi.org/10.1021/acssuschemeng.8b00981.
[23] M. Benitez-Guerrero, J.M. Valverde, P.E. Sanchez-Jimenez, A. Perejon, L.A. Perez-Maqueda, Multicycle activity of natural CaCO3 minerals for thermochemical energy storage in concentrated solar power plants, Sol. Energy 153 (2017) 188–199, https://doi.org/10.1016/j.solener.2017.05.068.
[24] L.M. Romeo, Y. Lara, P. Lisbona, A. Martínez, Economical assessment of competitive enhanced limestones for CO2 capture cycles in power plants, Fuel Process. Technol. 90 (2009) 803–811, https://doi.org/10.1016/j.fuproc.2009.03.014.
[25] J.M. Valverde, M. Barea-López, A. Perejón, P.E. Sánchez-Jiménez, L.A. Pérez-Maqueda, Effect of thermal pretreatment and nanosilica addition on limestone performance at calcium-looping conditions for thermochemical energy storage of concentrated solar power, Energy Fuels 31 (2017) 4226–4236, https://doi.org/10.1021/acs.energyfuels.6b03364.
[26] J. Chen, L. Duan, Z. Sun, Accurate control of cage-like CaO hollow microspheres for enhanced CO 2 capture in calcium looping via a template-assisted synthesis approach, Environ. Sci. Technol. 53 (2019) 2249–2259, https://doi.org/10.1021/acs.est.8b06138.
[27] F. Di Lauro, C. Tregambi, F. Montagnaro, P. Salatino, R. Chirone, R. Solimene, Improving the performance of calcium looping for solar thermochemical energy storage and CO2 capture, Fuel 298 (2021), 120791, https://doi.org/10.1016/j.fuel.2021.120791.
[28] F. Donat, N.H. Florin, E.J. Anthony, P.S. Fennell, Influence of high-temperature steam on the reactivity of CaO sorbent for CO 2 capture, Environ. Sci. Technol. 46 (2012) 1262–1269, https://doi.org/10.1021/es202679w.
[29] S. Champagne, D.Y. Lu, A. MacChi, R.T. Symonds, E.J. Anthony, Influence of steam injection during calcination on the reactivity of CaO-based sorbent for carbon capture, Ind. Eng. Chem. Res. 52 (2013) 2241–2246, https://doi.org/10.1021/ie3012787.
[30] V. Manovic, E.J. Anthony, Carbonation of CaO-based sorbents enhanced by steam addition, Ind. Eng. Chem. Res. 49 (19) (2010) 9105–9110, https://doi.org/10.1021/ie101352s.
[31] Z. Li, Y. Liu, N. Cai, Understanding the enhancement effect of high-temperature steam on the carbonation reaction of CaO with CO2, Fuel 127 (2014) 88–93, https://doi.org/10.1016/j.fuel.2013.06.040.
[32] H. Guo, S. Yan, Y. Zhao, X. Ma, S. Wang, Influence of water vapor on cyclic CO2 capture performance in both carbonation and decarbonation stages for Ca-Al mixed oxide, Chem. Eng. J. 359 (2019) 542–551, https://doi.org/10.1016/j.cej.2018.11.173.
[33] M. Kavosh, K. Patchigolla, E.J. Anthony, J.E. Oakey, Carbonation performance of lime for cyclic CO2 capture following limestone calcination in steam/CO2 atmosphere, Appl. Energy 131 (2014) 499–507, https://doi.org/10.1016/j.apenergy.2014.05.020.
[34] Y. Wang, S. Lin, Y. Suzuki, Limestone calcination with CO2 capture (II): decomposition in CO2/steam and CO2/N2 atmospheres, Energy Fuels 22 (2008) 2326–2331, https://doi.org/10.1021/ef800039k.
[35] S.L. Homsy, J. Moreno, A. Dikhtiarenko, J. Gascon, R.W. Dibble, Calcium looping: on the positive influence of SO2and the negative influence of H2O on CO2Capture by metamorphosed limestone-derived sorbents, ACS Omega 50 (2020) 32318, https://doi.org/10.1021/acsomega.0c04157.
[36] H. Lu, E.P. Reddy, P.G. Smirniotis, Calcium oxide based sorbents for capture of carbon dioxide at high temperatures, Ind. Eng. Chem. Res. 45 (2006) 3944–3949, https://doi.org/10.1021/ie051325x.
[37] P. Sun, J.R. Grace, C.J. Lim, E.J. Anthony, Investigation of attempts to improve cyclic CO2 capture by sorbent hydration and modification, Ind. Eng. Chem. Res. 47 (6) (2008) 2024–2032, https://doi.org/10.1021/ie070335q.
[38] L. Zhang, B. Zhang, Z. Yang, M. Guo, The role of water on the performance of calcium oxide-based sorbents for carbon dioxide capture: a review, Energy Technol. 3 (1) (2015) 10–19, https://doi.org/10.1002/ente.201402099.
[39] B.R. Stanmore, P. Gilot, Review-calcination and carbonation of limestone during thermal cycling for CO2 sequestration, Fuel Process. Technol. 86 (16) (2005) 1707–1743, https://doi.org/10.1016/j.fuproc.2005.01.023.
[40] R.H. Borgwardt, Calcium oxide sintering in atmospheres containing water and carbon dioxide, Ind. Eng. Chem. Res. 28 (1989) 493–500, https://doi.org/10.1021/ie00088a019.
[41] R.T. Symonds, D.Y. Lu, R.W. Hughes, E.J. Anthony, A. Macchi, CO2 capture from simulated syngas via cyclic carbonation/calcination for a naturally occurring limestone: pilot-plant testing, Ind. Eng. Chem. Res. 48 (18) (2009) 8431–8440, https://doi.org/10.1021/ie900645x.
[42] B. Dou, Y. Song, Y. Liu, C. Feng, High temperature CO2 capture using calcium oxide sorbent in a fixed-bed reactor, J. Hazard. Mater. 183 (2010) 759–765, https://doi.org/10.1016/j.jhazmat.2010.07.091.
[43] B. Arias, G. Grasa, J.C. Abanades, V. Manovic, E.J. Anthony, The effect of steam on the fast carbonation reaction rates of CaO, Ind. Eng. Chem. Res. 51 (5) (2012) 2478–2482, https://doi.org/10.1021/ie202648p.
[44] J.Jesús Arcenegui Troya, P.Enrique Sánchez-Jiménez, A. Perejón, V. Moreno, J. Manuel Valverde, L.Allan Pérez-Maqueda, Kinetics and cyclability of limestone (CaCO3) in presence of steam during calcination in the CaL scheme for thermochemical energy storage, Chem. Eng. J. 417 (2021) 129194, https://doi.org/10.1016/j.cej.2021.129194.
[45] E.E. Berger, Effect of steam on the decomposition of limestone, Ind. Eng. Chem. 19 (1927) 594–596, https://doi.org/10.1021/ie50209a026.
[46] Z.H. Li, Y. Wang, K. Xu, J.Z. Yang, S.B. Niu, H. Yao, Effect of steam on CaO regeneration, carbonation and hydration reactions for CO2 capture, Fuel Process. Technol. 151 (2016) 101–106, https://doi.org/10.1016/j.fuproc.2016.05.019.
[47] J. Yin, X. Kang, C. Qin, B. Feng, A. Veeraragavan, D. Saulov, Modeling of CaCO3 decomposition under CO2/H 2O atmosphere in calcium looping processes, Fuel Process. Technol. 125 (2014) 125–138, https://doi.org/10.1016/j.fuproc.2014.03.036.
[48] G. Giammaria, L. Lefferts, Catalytic effect of water on calcium carbonate decomposition, J. CO2 Util. 33 (2019) 341–356, https://doi.org/10.1016/j.jcou.2019.06.017.
[49] M. Silakhori, M. Jafarian, A. Chinnici, W. Saw, M. Venkataraman, W. Lipiński, G. J. Nathan, Effects of steam on the kinetics of calcium carbonate calcination, Chem. Eng. Sci. 246 (2021), 116987, https://doi.org/10.1016/j.ces.2021.116987.
[50] Y. Wang, W.J. Thomson, The effects of steam and carbon dioxide on calcite decomposition using dynamic X-ray diffraction, Chem. Eng. Sci. 50 (9) (1995) 1373–1382, https://doi.org/10.1016/0009-2509(95)00002-M.
[51] W.H. Maclntire, T.B. Stansel, Steam catalysis in calcinations of dolomite and limestone fines, Ind. Eng. Chem. 45 (1953) 1548–1555, https://doi.org/10.1021/ie50523a050.
[52] D. Dollimore, T.L. Shively, W.A. Kneller, F.W. Wilburn, The thermal decomposition of dolomite samples, in: Proc. Conf. North Am. Therm. Anal. Soc., 26th 165, 1998, pp. 217–218.
[53] S. Guo, H. Wang, D. Liu, L. Yang, X. Wei, S. Wu, Understanding the impacts of impurities and water vapor on limestone calcination in a laboratory-scale fluidized bed, Energy Fuels 29 (2015) 7572–7583, https://doi.org/10.1021/acs.energyfuels.5b01218.
[54] J.D. Durán-Martín, P.E. Sánchez Jimenez, J.M. Valverde, A. Perejón, J. Arcenegui-Troya, P. García Triñanes, L.A. Pérez Maqueda, Role of particle size on the multicycle calcium looping activity of limestone for thermochemical energy storage, J. Adv. Res. 22 (2020) 67–76, https://doi.org/10.1016/j.jare.2019.10.008.
[55] F.J. Durán-Olivencia, J.M.P. Ebri, M.J. Espín, J.M. Valverde, The cohesive behavior of granular solids at high temperature in solar energy storage, Energy Convers. Manag. 240 (2021), 114217, https://doi.org/10.1016/j.enconman.2021.114217.
[56] R. Gannoun, J.M.P. Ebrí, A.T. Pérez, M.J. Espín, F.J. Durán-Olivencia, J. M. Valverde, Nanosilica to improve the flowability of fine limestone powders in thermochemical storage units, Chem. Eng. J. 426 (2021), 131789, https://doi.org/10.1016/j.cej.2021.131789.
[57] P.E. Sanchez-Jimenez, J.M. Valverde, L.A. Perez-Maqueda, Multicyclic conversion of limestone at Ca-looping conditions: the role of solid-sate diffusion controlled carbonation, Fuel 127 (2014) 131–140, https://doi.org/10.1016/j.fuel.2013.09.064.
[58] J.M. Valverde, P.E. Sanchez-Jimenez, A. Perejon, L.A. Perez-Maqueda, CO2 multicyclic capture of pretreated/doped CaO in the Ca-looping process. Theory and

experiments, Phys. Chem. Chem. Phys. 15 (2013) 11775–11793, https://doi.org/10.1039/c3cp50480h.
[59] J. Arcenegui-Troya, P.E. Sánchez-Jiménez, A. Perejón, V. Moreno, J.M. Valverde, L.A. Pérez-Maqueda, Kinetics and cyclability of limestone (CaCO3) in presence of steam during calcination in the CaL scheme for thermochemical energy storage, Chem. Eng. J. 417 (2021), 129194, https://doi.org/10.1016/j.cej.2021.129194.
[60] B. Zhao, Y. Su, J. Zhang, Simulation of gas flow pattern and separation efficiency in cyclone with conventional single and spiral double inlet configuration, Chem. Eng. Res. Des. 84 (2006) 1158–1165, https://doi.org/10.1205/cherd06040.
[61] J.M. Valverde, M.A.S. Quintanilla, Attrition of Ca-based CO2-adsorbents by a high velocity gas jet, AIChE J. 59 (2013) 1096–1107, https://doi.org/10.1002/aic.13908.
[62] C. Ho, A review of high-temperature particle receivers for concentrating solar power, Appl. Therm. Eng. 109 (2016) 958–969, https://doi.org/10.1016/j.applthermaleng.2016.04.103.
[63] G. Zsembinszki, A. Solé, C. Barreneche, C. Prieto, A.I. Fernández, L.F. Cabeza, Review of reactors with potential use in thermochemical energy storage in concentrated solar power plants, Energies 11 (9) (2018) 2358, https://doi.org/10.3390/en11092358.
[64] C. Tregambi, M. Troiano, F. Montagnaro, R. Solimene, P. Salatino, Fluidized beds for concentrated solar thermal technologies—a review, Front. Energy Res. 9 (2021) 13, https://doi.org/10.3389/fenrg.2021.618421.
[65] B. Arias, M.E. Diego, J.C. Abanades, M. Lorenzo, L. Diaz, D. Martínez, J. Alvarez, A. Sánchez-Biezma, Demonstration of steady state CO2 capture in a 1.7 MWth calcium looping pilot, Int. J. Greenh. Gas Control. 18 (2013) 237.
[66] J. Ströhle, M. Junk, J. Kremer, A. Galloy, B. Epple, Carbonate looping experiments in a 1MWth pilot plant and model validation, Fuel 127 (2014) 13–22, https://doi.org/10.1016/j.fuel.2013.12.043.